Active Disturbance Rejection Control of Synchronous Reluctance Motors

Angelo Accetta[a], Maurizio Cirrincione[b], Filippo D'Ippolito[c], Marcello Pucci[a], Antonino Sferlazza[c]

[a]INstitute for Marine engineering (*INM*), section of Palermo, National Research Council of Italy (*CNR*), Via Ugo La Malfa 153, 90146 Palermo, Italy. (angelo.accetta@cnr.it, marcello.pucci@cnr.it)
[b]School of Engineering, University of the South Pacific, Laucala Campus, Suva, Fiji Islands. (m.cirrincione@ieee.org)
[c]Department of Engineering (*DI*), University of Palermo, viale delle scienze Ed. 10, 90128 Palermo, Italy. (filippo.dippolito@unipa.it, antonino.sferlazza@unipa.it)

***Abstract*— This paper proposes the theoretical framework and the experimental application of the Active Disturbance Rejection Control (*ADRC*) to Synchronous Reluctance Motor (*SynRM*) drives. The ADRC is a non-linear control technique which can be viewed as a particular kind of input-output Feedback Linearization Control (*FLC*), where the non-linear transformation of the state is not computed by means of the model, but is estimated on-line. This approach permits coping with unmodeled dynamics as well as uncertainty in the knowledge of the model parameters and exogenous disturbances. The effectiveness of the proposed control law has been verified experimentally on a suitably developed test set-up. Experimental results fully confirm the high dynamic performance guaranteed theoretically by ADRC.**

I. Introduction

The first prototypes of the synchronous reluctance motors (*SynRM*) date back to the first decades of 1900. At the very beginning, SynRMs were rarely adopted because of their low performance in terms of output torque and power, and their relatively high price. Nevertheless, over the last few years more performing SynRM have been designed and constructed with higher reliability and robustness, making them suitable for industry applications. In particular, improvements in rotor design have allowed increased saliency ratio ranging from 9 to 12 [1]. Indeed, high saliency ratios have permitted high performance applications, like machine tools drives, robotics, and electrical vehicles. Another possible application is in energy storage drives, like flywheel energy storage systems, especially of low power, as needed in small islands. Because of their construction characteristics, SynRMs can be hardly operated in open loop. High dynamic performance can be achieved by adopting vector control techniques and several rotor-oriented or stator flux-oriented control schemes have been developed [2]–[4]. Theoretically, the performance of the SynRMs is limited, however, by the strong magnetic non-linearity of the machine, with different self-saturation phenomena on the direct and quadrature axes, as well as significant cross-saturation phenomena. To address these issues, a large number of nonlinear control strategies are available [5], [6]. Nevertheless, few applications of nonlinear control methods to electrical drives are in general present in the scientific literature, and even less for SynRMs. Among these, one of the most promising nonlinear control strategies is the input-output feedback linearization (*FLC*) [7]–[11]. In particular, [8], [9] propose an adaptive input-output feedback-linearization (*AIOFL*) technique used for speed and torque-tracking control of a SynRM drive. [10] proposes a nonlinear controller, which is able to directly regulate the torque by selecting the product of direct and quadrature axes currents as one of the output variables. Recently, a nonlinear controller based on input-output FL for SynRMs drives has been presented, considering the self and cross-saturation saturation effects [12]. The space-vector dynamic model adopted for developing the proposed FLC technique has been proposed in [13], and the related magnetic model including both the self and cross-saturation has been described in [14]. The input-output FLC technique is, however, a model-based control, and therefore it suffers primarily from two disadvantages: 1) the accuracy of the dynamic model on which the control law is based; and 2) the corresponding correct knowledge of the model parameters. A way to deal with this problem is to design robust control techniques able to consider the parameter uncertainties explicitly: [15], [16]. Another very promising way to overcome these limitations of the FLC is the adoption of the active disturbance rejection control (*ADRC*) [17], [18]. In ADRC, the order of the dynamic model of the system to be controlled is augmented, considering the additional nonlinear function, permitting the system to be linearized, with an additional component of the state. While in the classic FLC this function is assumed to be known, in the ADRC this function is estimated on-line by means of an extended state observer (*ESO*). It follows that ADRC can be considered as an "*adaptive robust version*" of the FLC control technique, since the state feedback term is estimated on-line. In this way, not only are the problems due to uncertainties on the parameters addressed, but it is also possible to handle unmodeled dynamics and exogenous disturbances (like load torques). Specifically, this paper develops theoretically an ADRC control technique for SynRMs drives, in particular for those applications that require few perturbations in speed and torque loops. Indeed, flywheel energy storage systems require disturbance rejection to decrease the wear-out of the components and extend their life-time. The proposed ADRC has been tested experimentally on a suitably developed test set-up.

II. Space-vector state model considering self and cross-saturation

A novel complete magnetic model of the SynRM has been proposed in [14], where specific flux versus current functions have been deduced, permitting both the self and cross-saturation effects to be accounted for. Correspondingly, [13] has proposed a new space-vector model of the SynRM including self and cross-saturation effects, expressed in state form, written in the rotor reference frame. Both the complete magnet model and the state space representation of the model are briefly described in the following as an introduction to the proposed control strategy.

If $\mathbf{\Psi}_s = [\psi_{sx},\ \psi_{sy}]$ is the vector whose elements are the stator direct and quadrature flux components in the rotor reference frame, and $\mathbf{i}_s = [i_{sx},\ i_{sy}]$ is the corresponding stator current vector, the complete space-vector dynamic model of the SynRM in state form, selecting the stator fluxes as state variables, can be written as [14]:

$$\frac{d\mathbf{\Psi}_s}{dt} = \mathbf{u}_s - R_s\mathbf{i}_s - j\omega_r\mathbf{\Psi}_s. \tag{1}$$

As shown in [14], the stator fluxes can be obtained from the stator current by means of the following relations:

$$\psi_{sx} = L_{sxx}i_{sx}, \qquad \psi_{sy} = L_{syy}i_{sy}, \tag{2}$$

where the static inductance components are defined as follows:

$$L_{sxx} = \alpha\frac{1-e^{-ai_{sx}}}{|i_{sx}|} + \beta - \gamma\frac{1-e^{-bi_{sx}i_{sy}}}{i_{sx}^2}, \tag{3}$$

$$L_{syy} = \delta\frac{1-e^{-ci_{sy}}}{|i_{sy}|} + \epsilon - \gamma\frac{1-e^{-bi_{sx}i_{sy}}}{i_{sy}^2}, \tag{4}$$

The entire magnetic behavior of the machine can be, therefore, described by functions requiring the knowledge of 8 model parameters. In [14], it has been further shown that the functions (2) properly satisfy the reciprocity conditions as for the cross-saturation, ensuring that the nonlinear inductances do not generate or dissipate energy. Moreover, an identification technique of the saturation model obtained with stand-still tests and based on Genetic Algorithms (*GA*), without the need for locking the rotor, has been proposed and validated experimentally [14].

By using Eq.s (2)-(4), model (1) can be also conveniently written by considering the stator currents as state variables, instead of the stator fluxes, as follows:

$$\frac{d\mathbf{i}_s}{dt} = \mathbf{L}_s'^{-1}\left(\mathbf{u}_s - R_s\mathbf{i}_s - j\omega_r\mathbf{L}_s\mathbf{i}_s\right). \tag{5}$$

The inverse of the dynamic inductances matrix $\mathbf{L}_s'$ in (5) is defined as:

$$\mathbf{L}_s'^{-1} = \frac{1}{L'_{sxx}L'_{syy} - L'_{sxy}L'_{syx}}\begin{bmatrix} L'_{sxx} & L'_{syx} \\ L'_{sxy} & L'_{syy}\end{bmatrix}, \tag{6}$$

where the self and cross dynamic inductances can be retrieved as follows:

$$L'_{sxx} = \frac{d\psi_{sx}}{di_{sx}} = \alpha a e^{-ai_{sx}} + \beta - \gamma\frac{(1+bi_{sx}i_{sy})e^{-bi_{sx}i_{sy}} - 1}{i_{sx}^2} \tag{7}$$

$$L'_{syy} = \frac{d\psi_{sy}}{di_{sy}} = \delta c e^{-ci_{sx}} + \epsilon - \gamma\frac{(1+bi_{sx}i_{sy})e^{-bi_{sx}i_{sy}} - 1}{i_{sy}^2} \tag{8}$$

$$L'_{sxy} = L'_{syx} = \frac{d\psi_{sx}}{di_{sy}} = \frac{d\psi_{sy}}{di_{sx}} = \gamma b e^{-bi_{sx}i_{sy}} \tag{9}$$

Finally the mechanical equation of the SynRM is given by:

$$J\frac{d\omega_r}{dt} = -f_v\omega_r + t_m - t_l, \tag{10}$$

where J and f_v are the inertia moment and the viscous friction coefficient, t_l is the load torque, and t_m is the electromagnetic torque generated by the motor and given by:

$$t_m = \frac{3}{2}p\left(L_{sxx} - L_{syy}\right)i_{sx}i_{sy} = \frac{3}{2}p\left(\frac{1}{L_{sxx}} - \frac{1}{L_{syy}}\right)\psi_{sx}\psi_{sy}. \tag{11}$$

It is noteworthy that, only the expression of the static inductances appears in the dynamics of the speed, since the electromagnetic torque depends explicitly on static inductances, and depends on dynamic inductances only indirectly through stator fluxes.

III. The active disturbance rejection control law

The proposed ADRC technique is based on the construction of an extended model of order $n+1$, where n is the order of the system to be controlled. An additional state variable should be introduced to represent the total disturbance due to parameter uncertainties, external disturbances and non-linearities. The model is eventually expressed in a canonical form with a chain of integrators. On this basis, an ESO is to be designed to estimate the total disturbance. Finally, a control law is determined consisting of two components: the first compensates the total disturbance and the second provides the desired behavior to the system.

A. Extended models

Two distinct extended models are proposed, i.e. the flux extended model and the speed extended model. The first consists of the equations of the model described in Section II expressing the dynamics of the the flux on the x axis, ψ_{sx}. The other consists of the equations expressing the dynamics of the mechanical speed ω_r.

1) Flux extended model: From model (1)-(5), using the linearization procedure used in [12], and defining $x_{\psi_1} = \psi_{sx}$, the following equation can be written:

$$\dot{x}_{\psi_1} = f_\psi + u_{sx}. \tag{12}$$

where f_ψ is called *total flux disturbance* defined as follows:

$$f_\psi = -R_s i_{sx} + \omega_r\psi_{sy}. \tag{13}$$

Now if an extra state variable $x_{\psi_2} = f_\psi$ is defined, the flux extended model becomes:

$$\dot{x}_{\psi_1} = x_{\psi_2} + u_{sx}, \qquad \dot{x}_{\psi_2} = \dot{f}_\psi. \tag{14}$$

2) Speed extended model: The procedure used for obtaining the speed extended model parallels the one used to definine the flux extended model, but in this case the speed is assumed as a measured output. In this case, from the model equations (1)-(5) and (10)-(11), using the linearization procedure used in [12], and defining $x_{\omega 1} = \omega_r$ and $x_{\omega 2} = \dot{\omega}_r = a$, the following equations can be written:

$$\dot{x}_{\omega 1} = x_{\omega 2}, \qquad \dot{x}_{\omega 2} = f_\omega + b_\omega u_{sy}, \tag{15}$$

where f_ω is called *total speed disturbance* defined as follows:

$$f_\omega = -f_v a + \frac{3p}{2J}\Bigg(\begin{bmatrix} g_1 & g_2 \end{bmatrix} {\mathbf{L}'_s}^{-1} + \left(\frac{1}{L_{sxx}} - \frac{1}{L_{syy}}\right)\begin{bmatrix}\psi_{sx} & \psi_{sy}\end{bmatrix}\Bigg)\begin{bmatrix} u_{sx} - R_s i_{sx} + \omega_r \psi_{sy} \\ -R_s i_{sy} - \omega_r \psi_{sx}\end{bmatrix}, \tag{16}$$

where:

$$g_1 := \left(\frac{\frac{\partial L_{sxx}}{\partial i_{sx}}}{L_{sxx}^2} - \frac{\frac{\partial L_{syy}}{\partial i_{sx}}}{L_{syy}^2}\right) = \frac{1}{i_{sx}}\left(\frac{L'_{sxx} - L_{sxx}}{L_{sxx}^2}\right) + \frac{1}{i_{sy}}\left(\frac{L'_{syx}}{L_{syy}^2}\right), \tag{17a}$$

$$g_2 := \left(\frac{\frac{\partial L_{sxx}}{\partial i_{sy}}}{L_{sxx}^2} - \frac{\frac{\partial L_{syy}}{\partial i_{sy}}}{L_{syy}^2}\right) = \frac{1}{i_{sy}}\left(\frac{L'_{syy} - L_{syy}}{L_{syy}^2}\right) + \frac{1}{i_{sx}}\left(\frac{L'_{sxy}}{L_{sxx}^2}\right). \tag{17b}$$

while b_ω is defined as:

$$b_\omega = \frac{3p}{2J}\left(\frac{g_1 L'_{sxy} + g_2 L'_{syy}}{L'_{sxx} L'_{syy} - {L'_{sxy}}^2} + \left(\frac{1}{L_{syy}} - \frac{1}{L_{sxx}}\right)\psi_{sx}\right). \tag{18}$$

Also in this case, if an extra state variable $x_{\omega 3} = f_\omega$ is defined, the speed extended model becomes:

$$\dot{x}_{\omega 1} = x_{\omega 2}, \qquad \dot{x}_{\omega 2} = x_{\omega 3} + b_\omega u_{sy}, \qquad \dot{x}_{\omega 3} = \dot{f}_\omega. \tag{19}$$

Models (14) and (19) show that the flux and speed extended models have the same structure, but different dimensions. Moreover, choosing the control variables as follows:

$$u_{sx} = -\hat{x}_{\psi 2} + \nu'_x, \qquad u_{sy} = \frac{1}{b_\omega}\left(-\hat{x}_{\omega 3} + \nu'_y\right), \tag{20}$$

where $\hat{x}_{\psi 2}$ and $\hat{x}_{v3}$ are the estimates of $x_{\psi 2}$ and x_{v3}, respectively, and designing ν'_x and ν'_y so that the models (14) and (19) satisfy the design requirements, the total disturbances can be assumed as perfectly compensated. The total disturbances can be estimated with two ESOs. In particular two ESOs will be designed to estimate the state of the extended models and, as can be easily viewed from the model, the estimate of the total disturbance corresponds to the estimate of the second state variable for the flux model and of the third state variable for the speed model.

Remark 1: On the basis of the above, the differences between the classic FL and the proposed ADRC technique are clear. Indeed, in the FL shown in [12] the control inputs are designed as in (20), but the total disturbances $f_\psi = x_{\psi 2}$ and $f_\omega = x_{\omega 3}$ are analytically computed as in (13) and (16) with a drawback arising from the uncertainties on the parameters due to the complexity of the formulation of (13) and (16). With the proposed ADRC, these terms are estimated as shown in the following, and no knowledge on the structure of these terms is needed. In this way, not only are the problems of parameter uncertainty addressed, but also possible issues from unmodelled dynamics are addressed.

B. ESO for a third-order extended model

In the following, ESOs for both speed and flux extended model will be considered. Note that flux and speed extended models have the same structure but different dimensions: this means that all the calculations and considerations given for one model can be easily adapted to the other extended model.

The ESO chosen for the state estimation of model (19) is that proposed in [19], whose set of equations is given by:

$$\dot{\hat{x}}_{\omega 1} = \hat{x}_{\omega 2} - \epsilon h_1\left(\frac{\hat{x}_{\omega 1} - x_{\omega 1}}{\epsilon^2}\right), \tag{21a}$$

$$\dot{\hat{x}}_{\omega 2} = \hat{x}_{\omega 3} - h_2\left(\frac{\hat{x}_{\omega 1} - x_{\omega 1}}{\epsilon^2}\right) + b_\omega u_{sy}, \tag{21b}$$

$$\dot{\hat{x}}_{\omega 3} = -\epsilon^{-1} h_3\left(\frac{\hat{x}_{\omega 1} - x_{\omega 1}}{\epsilon^2}\right), \tag{21c}$$

where ϵ is a suitable positive parameter, and the functions $h_i(\cdot)$, $i = 1, 2, 3$, can be either linear or non-linear functions.

Defining the estimation errors:

$$\eta_i = \frac{e_i}{\epsilon^{3-i}},\ i = 1, 2, 3, \tag{22}$$

the dynamics of the variables η_i are described by the equations:

$$\epsilon\dot{\eta}_1 = \eta_2 - h_1(\eta_1),\ \epsilon\dot{\eta}_2 = \eta_3 - h_2(\eta_1),\ \epsilon\dot{\eta}_3 = -\epsilon\dot{h} - h_3(\eta_1). \tag{23}$$

The structure of $h_i(\eta_1)$, $i = 1, 2, 3$, characterizes the ESO. This paper considers the Linear ESO (*LESO*). With this choice, fixing $h_i(\eta_1) = \beta_i \eta_1$, $i = 1, 2, 3$, with β_i positive constants, equations (23) can be written as follow:

$$\epsilon\dot{\boldsymbol{\eta}} = \boldsymbol{A}\boldsymbol{\eta} + \epsilon\boldsymbol{b}\dot{f}_\omega \tag{24}$$

where $\boldsymbol{\eta} = \begin{bmatrix}\eta_1 & \eta_2 & \eta_3\end{bmatrix}^T$, $\boldsymbol{A} = \begin{bmatrix} -\beta_1 & 1 & 0 \\ -\beta_2 & 0 & 1 \\ -\beta_3 & 0 & 0\end{bmatrix}$, and $\boldsymbol{b} = \begin{bmatrix}0 & 0 & -1\end{bmatrix}^T$.

In [19] it is shown that if coefficients β_i are chosen such that matrix $\boldsymbol{A}$ is Hurwitz, and if the derivative of the total speed disturbance is bounded, or rather if there exists a positive constant P such that $|\dot{f}_\omega| < P$, then the estimation errors (22) converge to zero exponentially.

For the flux extended model, the same calculations can be done but considering a second order dynamics instead of a third order one. For this reason, the ESO chosen for the state

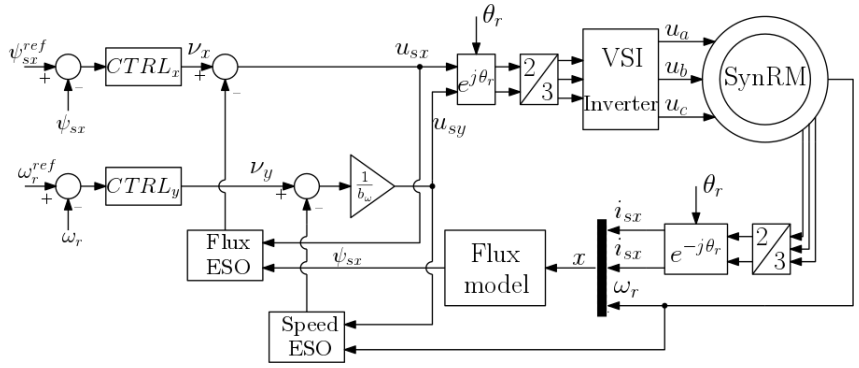

Figure 1. Block diagram of the proposed control algorithm.

estimation of model (15) is given by:

$$\dot{\hat{x}}_{\psi_1} = \hat{x}_{\psi_2} - h_1\left(\frac{\hat{x}_{\psi_1} - x_{\psi_1}}{\epsilon}\right) + b_\psi u_{sx}, \tag{25a}$$

$$\dot{\hat{x}}_{\psi_2} = -\epsilon^{-1} h_2\left(\frac{\hat{x}_{\psi_1} - x_{\psi_1}}{\epsilon}\right), \tag{25b}$$

where ϵ is a suitable positive parameter, and the functions $h_i(\cdot)$, $i = 1, 2$, are chosen as linear terms like the speed ESO.

C. Design of flux and speed controllers

With reference to (19), if the control input is selected as in equation (20), and considering that $\hat{x}_{\omega 3} \approx x_{\omega 3}$, then the following model is obtained:

$$\dot{x}_{\omega 1} = x_{\omega 2}, \qquad \dot{x}_{\omega 2} = \nu_y'. \tag{26}$$

This structure corresponds to a double integrator (if the flux model is considered, a single integrator is obtained: $\dot{x}_{\psi_1} = \nu_x'$). This model is reachable and, consequently, a state feedback control law based on the assignment of the eigenvalues can be derived, but it does not allow steady-state null tracking errors to be obtained. As a result, to have perfect tracking of constant reference, the state of model (26) is augmented by adding a third variable z, whose dynamics is:

$$\dot{z}_\omega = x_{1\omega ref} - x_{\omega 1}, \tag{27}$$

where $x_{1\omega ref}$ is the desired value of speed. It is easy to verify that model (26)-(31) is reachable and the control law:

$$\nu_y' = -\boldsymbol{k}_\omega^T \boldsymbol{x}, \tag{28}$$

with $\boldsymbol{k}_\omega = \begin{bmatrix} k_{\omega 1} & k_{\omega 2} & k_{\omega 3} \end{bmatrix}^T$ and $\boldsymbol{x} = \begin{bmatrix} x_{\omega 1} & x_{\omega 2} & z_\omega \end{bmatrix}^T$, allows the eigenvalues of the dynamic matrix of the model to be assigned. The characteristic polynomial is given by:

$$\Delta(\lambda) = \lambda^3 + k_{\omega 1}\lambda^2 + k_{\omega 2}\lambda + k_{\omega 3}, \tag{29}$$

where the parameters $k_{\omega 1}$, $k_{\omega 2}$ and $k_{\omega 3}$ are determined assuming that the desired eigenvalues are $\lambda_{\omega 1} = -\zeta\omega_n + j\omega_n\sqrt{1-\zeta^2}$, $\lambda_{\omega 2} = -\zeta\omega_n - j\omega_n\sqrt{1-\zeta^2}$ and $\lambda_{\omega 3} = \sigma$, where ω_n and ζ are the natural frequency and the damping factor respectively, while σ is a negative real number. Obviously, the implementation of the above control law can be carried out using the state estimated by the ESO. More precisely, the implementation of the control law requires the knowledge of $x_{\omega 1}$ and $x_{\omega 2}$, while the knowledge of $x_{\omega 3}$ allows the total disturbance f_ω to be compensated.

With reference to the controller design for the flux model (19), the same procedure given above for the speed controller can be followed. In particular, if the control input is selected as in equation (20), and considering that $\hat{x}_{\psi_2} \approx x_{\psi_2}$, then the following model is obtained:

$$\dot{x}_{\psi_1} = \nu_x' \tag{30}$$

This structure corresponds to an integrator, which is reachable and, consequently, a state feedback control law based on the assignment of the eigenvalues can be derived. Also in this case, for obtaining a steady-state null error the state is augmented by adding a second variable z_ψ, whose dynamics is:

$$\dot{z}_\psi = x_{1\psi_{ref}} - x_{\psi_1}, \tag{31}$$

where $x_{1\psi_{ref}}$ is the desired flux. Thus, the control law:

$$\nu_x' = -\boldsymbol{k}_\psi^T \boldsymbol{x}, \tag{32}$$

with $\boldsymbol{k}_\psi = \begin{bmatrix} k_{\psi 1} & k_{\psi 2} \end{bmatrix}^T$ and $\boldsymbol{x} = \begin{bmatrix} x_{\psi_1} & z_\psi \end{bmatrix}^T$, allows the eigenvalues of the dynamic matrix of the model to be assigned. In this case, parameters $k_{\psi 1}$, $k_{\psi 2}$ are determined by assuming that the desired eigenvalues are $\lambda_{\psi 1} = -\zeta\omega_n + j\omega_n\sqrt{1-\zeta^2}$ and $\lambda_{\psi 2} = -\zeta\omega_n - j\omega_n\sqrt{1-\zeta^2}$, where ω_n and ζ are the natural frequency and the damping factor respectively.

The block diagram of the proposed control algorithm is shown in Fig. 1.

Remark 2: Note that the proposed control scheme requires the existence of the inverse of b_ω. However, it is possible to prove that the inverse exists if $\psi_{sx} \neq 0$ and this condition is always satisfied because the SynRM works properly only if the flux ψ_{sx} is strictly greater than zero for any working condition, meaning that the machine is properly magnetized.

Remark 3: Note that here the auxiliary input ν_x appears in the definition of the total disturbance f_ω, that made the proposed scheme nonconventional, since it has never been considered and tested in past works. This problem aries from the dependency of the self and cross-saturation inductances of the model on the stator current.

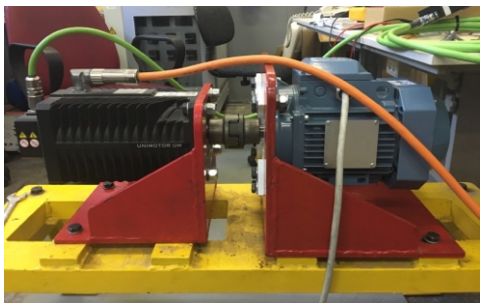

Figure 2. Photograph of the SynRM experimental set-up.

Table I
PARAMETERS OF THE SYNRM SATURATION MODEL

SYMBOLS	VALUES
a	0.35
b	4.04
c	1.20
α	0.35
β	0.0047
γ	0.0018
δ	0.13
ϵ	0.025

IV. TEST SET-UP

The proposed ADRC control technique has been tested experimentally on a suitably developed test set-up with the SynRM motor model ABB 3GAL092543-BSB with rated power 2.2 kW, rated speed 1500 rpm, rated torque of 14 Nm, rated current 5.5 A. The SynRM is mechanically coupled with a torque-controlled permanent magnet synchronous motor (*PMSM*) drive working as an active load. The SynRM is supplied by a Voltage Source Inverter (*VSI*) with insulated gate bipolar transistor (*IGBT*) modules, model Semikron SMK 50 GB 123, driven by a Space-Vector Pulse Width Modulation technique (*SV-PWM*) with PWM frequency set to 5 kHz. Fig. 2 shows the photo of the SynRM drive test set-up, and Tab. I shows the parameters of the complete saturation model, identified with the technique proposed in [14].

V. EXPERIMENTAL RESULTS

To verify the effectiveness of the proposed ADRC control technique and its dynamic performance, three kinds of experimental tests have been done: 1) start-up test at no load, 2) speed reversal at no load, 3) step load torque at constant speed.

As for test 1, a step speed reference of 50 rad/s has been given to the SynRM drive at no load. Fig. 3.a shows the reference and measured speeds, and the speed tracking error. It can be observed that the ADRC control works properly, ensuring high dynamic performance; the measured speed tracks the reference properly, and the steady-state speed is reached in almost 0.25 s. Fig. 3.b shows the direct and quadrature components of the stator currents expressed in the rotor reference frame, i_{sx} and i_{sy}, during the same test. It can be noted that i_{sx} is controlled to a constant value, almost equal to 2 A, while i_{sy} exhibits a stepwise waveform during the speed transient needed to generate the maximum propulsive torque. It can be also noted a limited non-null value at steady-state, needed to cover the friction torque of the drive.

As for test 2, a step speed reversal from -50 rad/s to 50 rad/s has been commanded at no load. Fig.s 3.c and 3.d show the same kind of waveforms shown as for test 1. The speed waveform clearly shows that the SynRM drive is able to properly perform the speed reversal with high dynamic performance, with the complete reversal accomplished in less than 0.25 s. In consistency with this, i_{sx} is controlled to a constant value, almost equal to 2 A, and i_{sy} exhibits a stepwise waveform during the speed reversal.

As for test 3, the SynRM drive runs at the constant speed reference equal to 50 rad/s; a positive square load profile of peak value equal to 5 Nm, followed by a negative one of the same peak value, has been applied to the drive by acting on the PMSM drive torque reference. Fig.s 3.e and 3.f show waveforms similar to those obtained in tests 1 and 2. The speed waveform shows the torque rejection capability of the ADRC control; indeed, as soon as the load torque is applied, the control immediately reacts and drives the speed back to the reference value, regardless the sign of the applied torque. Finally, Fig. 4 shows the load and the electromagnetic torques obtained. It should be remarked that the electromagnetic torque tracks the load torque quickly, during each transient, permitting the speed to be maintained at the reference value.

VI. ACKNOWLEDGMENT

This paper has been supported by the project REFEPICS2 (Design of a REnewable energy source system with a Flywheel Energy storage system for supplying energy in Small Pacific Islands on the Pacific with weak grid, PART2), funded by the French "Ministère des Affaires Etrangères et du Développement International (*MAEDI*)".

VII. CONCLUSION

The main contribution of this paper consists in the theoretical development and the experimental application of the ADRC of SynRM. The ADRC is a particular non-linear control technique: it can be considered as a particular kind of FLC, where the non-linear transformation of the state is estimated on-line rather than computed by means of the model. This approach addresses the unmodelling dynamics as well as uncertain model parameters and exogenous disturbances. The effectiveness of the proposed control law has been verified experimentally on a suitably developed test set-up. Experimental results fully confirm the high dynamic performance ensured theoretically by ADRC. The disturbance rejection obtained in this way can be applied to flywheel energy storage systems. This is the focus of current research with particular attention to storage systems for remote areas or small islands.

REFERENCES

[1] P. Vas, *Sensorless vector and direct torque control*. Oxford university press Oxford, UK, 1998.

[2] L. Xu, X. Xu, T. A. Lipo, and D. W. Novotny, "Vector control of a synchronous reluctance motor including saturation and iron loss," *IEEE Transactions on Industry Applications*, vol. 27, no. 5, pp. 977–985, 1991.

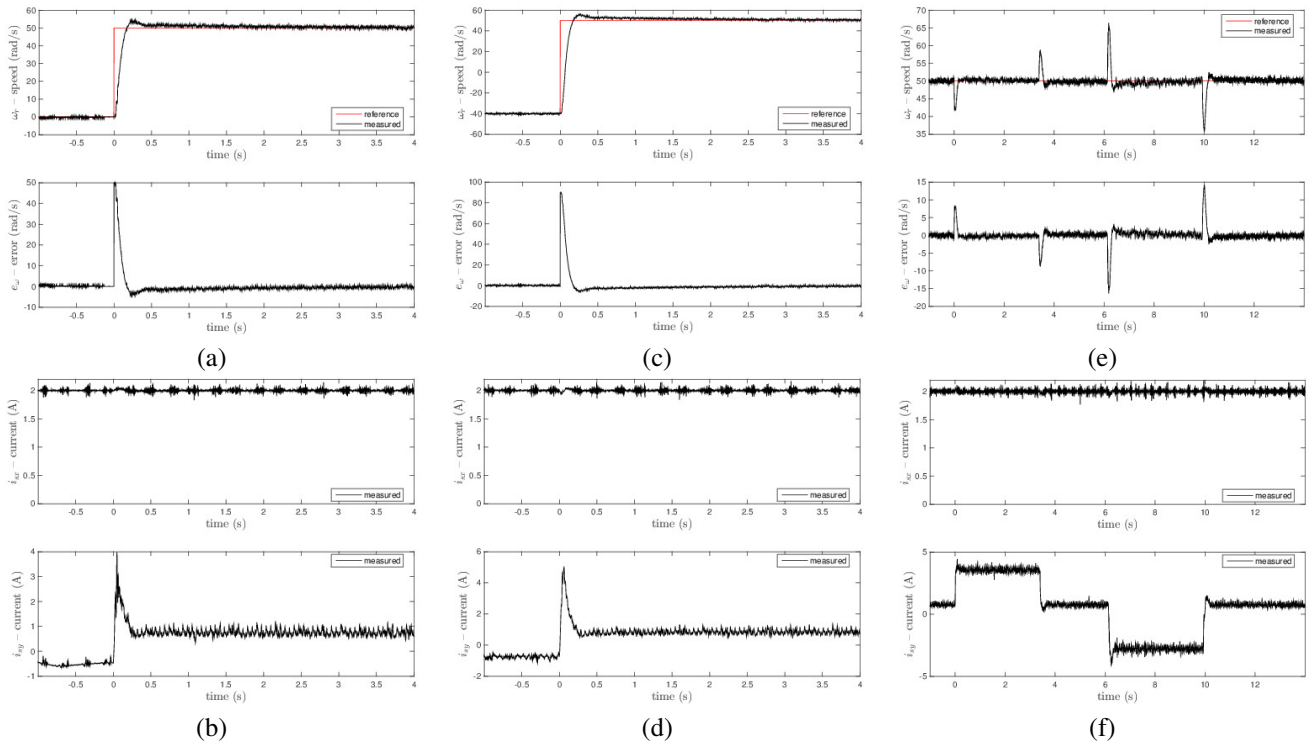

Figure 3. Reference and measured speed and i_{sx} and i_{sy} current component during: a set of torque steps (a)-(b), a speed reversal (c)-(d), a set of torque steps (e)-(f) (experiment).

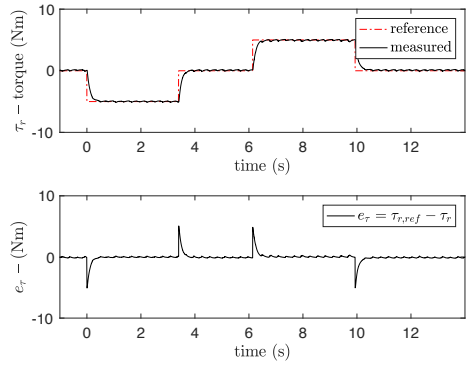

Figure 4. Reference and measured torque during a set of torque steps.

[3] R. E. Betz, R. Lagerquist, M. Jovanovic, T. J. Miller, and R. H. Middleton, "Control of synchronous reluctance machines," *IEEE Transactions on Industry Applications*, vol. 29, no. 6, pp. 1110–1122, 1993.

[4] A. Vagati, M. Pastorelli, and G. Franceschini, "High-performance control of synchronous reluctance motors," *IEEE Transactions on Industry Applications*, vol. 33, no. 4, pp. 983–991, 1997.

[5] H. K. Khalil, *Nonlinear systems*. Prentice hall, 2002, vol. 3.

[6] A. Isidori, *Nonlinear control systems, (third edition)*. Springer, 1995.

[7] K. A. Maa, B. Arundhati, and M. P. Kumar, "Design, performance of the speed control of a nonlinear variable reluctance motor drive using exact feedback linearization," in *Annual India Conference*, vol. 1. IEEE, 2008, pp. 57–64.

[8] H. A. Zarchi, J. Soltani, A. Maleknia, and G. R. A. Markadeh, "A Lyapunov based nonlinear speed tracking controller for synchronous reluctance motor using adaptive input-output feedback linearization technique," in *Conf. on Industrial Technology*. IEEE, 2008, pp. 1–5.

[9] H. A. Zarchi, J. Soltani, and G. A. Markadeh, "Adaptive input–output feedback-linearization-based torque control of synchronous reluctance motor without mechanical sensor," *IEEE Transactions on Industrial Electronics*, vol. 57, no. 1, pp. 375–384, 2010.

[10] H.-D. Lee, S.-J. Kang, and S.-K. Sul, "Efficiency-optimized direct torque control of synchronous reluctance motor using feedback linearization," *IEEE Transactions on Industrial Electronics*, vol. 46, no. 1, pp. 192–198, 1999.

[11] M. Nabipour, H. A. Zarchi, and S. Madani, "Robust position control of synchronous reluctance motor drives using linear variable structure and adaptive input-output feedback linearization approaches," in *Iranian Conference on Electrical Engineering*. IEEE, 2011, pp. 1–5.

[12] A. Accetta, M. Cirrincione, M. Pucci, and A. Sferlazza, "A nonlinear control of synchronous reluctance motors (SynRM) based on feedback linearization considering the self and cross-saturation effects," in *Energy Conversion Congress and Exposition*. IEEE, 2019, pp. 1804–1809.

[13] ——, "A space-vector state dynamic model of the synchronous reluctance motor including self and cross-saturation effects and its parameters estimation," in *Energy Conversion Congress and Exposition*. IEEE, 2018, pp. 4466–4472.

[14] ——, "A saturation model of the synchronous reluctance motor and its identification by genetic algorithms," in *Energy Conversion Congress and Exposition*. IEEE, 2018, pp. 4460–4465.

[15] A. Accetta, F. Alonge, M. Cirrincione, F. D'Ippolito, M. Pucci, R. Rabbeni, and A. Sferlazza, "Robust control for high performance induction motor drives based on partial state-feedback linearization," *IEEE Transactions on Industry Applications*, vol. 55, no. 1, pp. 490–503, 2018.

[16] F. Alonge, M. Cirrincione, M. Pucci, and A. Sferlazza, "A nonlinear observer for rotor flux estimation of induction motor considering the estimated magnetization characteristic," *IEEE Transactions on Industry Applications*, vol. 53, no. 6, pp. 5952–5965, 2017.

[17] J. Han, "From PID to active disturbance rejection control," *IEEE transactions on Industrial Electronics*, vol. 56, no. 3, pp. 900–906, 2009.

[18] Y. Huang and W. Xue, "Active disturbance rejection control: methodology and theoretical analysis," *ISA transactions*, vol. 53, no. 4, pp. 963–976, 2014.

[19] B.-Z. Guo and Z.-l. Zhao, "On the convergence of an extended state observer for nonlinear systems with uncertainty," *Systems & Control Letters*, vol. 60, no. 6, pp. 420–430, 2011.